Numerical investigations of endwall film cooling design of a turbine vane using four-holes pattern

Jian Liu
Department of Aeronautics and Astronautics, Central South University, Changsha, China

Mengyao Xu
Central South University, Changsha, China

Wenxiong Xi
Department of Aeronautics and Astronautics, Central South University, Changsha, China

Jiawen Song and Shibin Luo
Central South University, Changsha, China, and

Bengt Ake Sunden
Department of Energy Sciences, Lund University, Lund, Sweden

Abstract

Purpose – Endwall film cooling protects vane endwall by coolant coverage, especially at the leading edge (LE) region and vane-pressure side (PS) junction region. Strong flow impingement and complex vortexaa structures on the vane endwall cause difficulties for coolant flows to cover properly. This work aims at a full-scale arrangement of film cooling holes on the endwall which improves coolant efficiency in the LE region and vane-PS junction region.

Design/methodology/approach – The endwall film holes are grouped in four-holes constructal patterns. Three ways of arranging the groups are studied: based on the pressure field, the streamlines or the heat transfer field. The computational analysis is done with the k-ω SST model after validating the turbulence model properly.

Findings – By clustering the film cooling holes in four-holes patterns, the ejection of the coolant flow is stronger. The four-holes constructal patterns also improve the local coolant coverage in the "tough" regions, such as the junction region of the PS and the endwall. The arrangement based on streamlines distribution can effectively improve the coolant coverage and the arrangement based on the heat transfer distribution (HTD) has benefits by reducing high-temperature regions on the endwall.

Originality/value – A full-scale endwall film cooling design is presented considering interactions of different film cooling holes. A comprehensive model validation and mesh independence study are provided. The cooling holes pattern on the endwall is designed as four-holes constructal patterns combined with several arrangement choices, i.e. by pressure, by heat transfer and by streamline distributions.

Keywords Heat transfer, Coolant coverage, Endwall film cooling, Four-holes constructal pattern

Paper type Research paper

Nomenclature

Latin characters
C = chord of the vane (m);
d = interval between rows of cooling holes (m);
D = hole diameter (m);
F = film holes mass flow rate ratio;
k = turbulent kinetic energy (m^2/s^2);
M = mass flow rate ratio;
P = pitch between adjacent vanes (m);
S = slot mass flow rate ratio;
T = temperature (K);
u = velocity (m/s);
x = streamwise direction (m);
y = spanwise direction (m); and
z = normal direction (m).

Greek symbols
α = injection angle (°);
η = film cooling effectiveness, and
ρ = fluid density (kg/m^3).

Subscripts
c = coolant;
F = film cooling holes;
g = hot gas;
m = average/overall;
w = wall, and
S = slot.

Abbreviations
HTCD = heat transfer coefficient distributions;
LE = leading edge;
PD = pressure distributions;
PS = pressure side;
SD = streamlines distributions;
SS = suction side, and
TKE = turbulence kinetic energy.

1. Introduction

Film cooling is a common cooling method for gas turbine blades by ejecting a coolant from discrete holes and protect the solid surfaces. The great advantage of film cooling is that the coolant air uses the compressed air from the compressor and reduces the

surface temperature effectively though it may affect the aerodynamics. Great efforts have been put into the research works of film cooling in the past few decades (Han and Ekkad, 2001). The research works about film cooling have accumulated a large amount of literature, such as the shape optimization and location arrangement of the cooling holes (Ekkad and Han, 2013). For the geometrical effects of film cooling holes, research works are mainly focused on improving the coolant coverage on the solid surface, such as compound angle film cooling holes and cooling holes with a trench (Sundaram and Thole, 2008; Sundaram and Thole, 2009). In addition, some works pay attention to the operating conditions of the film cooling, such as effects of blowing ratio, density ratio, pressure ratio, temperature ratio and turbulence intensity. Recently, the investigations about film cooling for turbine blades are performed in a regime which tries to approach the reality, such as film cooling on a complex structured surface and the interaction of film cooling holes on a blade surface (Nemdili et al., 2011).

Some research works about film cooling are fundamental studies which are performed on a flat plate and concentrate on one parameter by isolating the effects of other parameters (Natsui et al., 2017; Wang et al., 2019; Zhang et al., 2019; Hou et al., 2019). Natsui et al. (Natsui et al., 2017) measured the adiabatic film cooling effectiveness (η) on a flat surface with multi-row arrays of film cooling holes by pressure-sensitive paint (PSP) method. With a thorough boundary layer analysis obtained by hotwire anemometry, the interaction of multi-row film cooling arrays is presented. Wang et al. (Wang et al., 2019) investigated the blowing ratio and density ratio of a flat plate film cooling effectiveness. They built correlations of film cooling for two rows of inline and staggered compound angled cylindrical holes.

For film cooling on the endwall between turbine vanes, exhaust gas impinges on the vanes and complex flow fields are formed, including horse-shoe and passage vortices (Langston, 1980). The complex flow structures have influences on coolant coverage on the endwall especially at the LE region and vane-PS junction region and the findings based on flat plate cannot be directly referred (Friedrichs et al., 1996). Therefore, many research works about endwall film cooling are conducted in a annular cascade or linear cascade. An early study about film cooling on the endwall in a linear cascade was carried out by Granser and Schulenberg (Granser and Schulenberg, 1990) in 1990. After that, a lot of works about endwall film cooling design has been performed (Oke et al., 2000; Oke et al., 2001; Zhang and Jaiswal, 2001; Knost and Thole, 2004; Ghosh and Goldstein, 2011; Shiau et al., 2016; Shiau et al., 2019; Yang et al., 2019; Chen et al., 2020; Chen et al., 2020; Liu et al., 2021). Simon et al. (Oke et al., 2001) performed a series of measurements for the film cooling on a contoured endwall. The flow measurement included normal flow field measurements and injection flow measurements. In their work, the migration of bleed flow and the interaction of passage flow and bleed flows were presented. At higher coolant flow rates, no suction-side coolant migration was found and strong blockage and mixing effect become obvious. Zhang and Jaiswal (Zhang and Jaiswal, 2001) investigated the endwall film cooling study using the PSP technique. However, the cooling holes were arranged upstream of the LE of the vane with a single row of discrete slots or a double staggered row of holes. From their work, high film cooling effectiveness could only be found when the cooling flows had higher mass flow ratios and dominated the endwall flow. Knost and Thole (Knost and Thole, 2004) measured the film cooling effectiveness on the endwall of a first stage vane. In their work, two kinds of film cooling patterns were measured. They found that there are two severe regions for the

coolant flow to cover, i.e. LE and PS-endwall junction region. Ghosh and Goldstein (Ghosh and Goldstein, 2011) investigated the inlet skew on the heat transfer and fluid flow on a turbine blade. The inlet skew is used to simulates the relative motion between the rotor and stator endwall. It showed that the inlet skew had a great effect on the pressure side (PS) due to interaction with the passage vortex. Shiau *et al*. (Shiau *et al*., 2016; Shiau *et al*., 2019) presented full-scale turbine vane endwall effectiveness contours using a PSP technique. The film cooling effectiveness (η) on the vanes placed in an annular-sector cascade was studied. The film cooling design contains a lot of shaped cooling holes dispersed on the vane and endwalls aiming to show the interaction of coolant flows with mainstream. The high-quality measurements by the PSP technique supported the promise of PSP in measuring the film cooling effectiveness. Yang *et al*. (Yang *et al*., 2019) investigated the conjugation heat transfer for the vane endwall considering the effect of upstream purge flow. They found the results indicate that purge flow has improved effects on endwall overall cooling effectiveness, particularly improving uniformity of temperature field. Chen *et al*. (Chen *et al*., 2020; Chen *et al*., 2020) investigated the full coverage film cooling design on a contoured endwall. The film cooling holes are designed as five rows perpendicular to the streamwise direction separated on the endwall. They found the contoured endwall has better performance than the flat endwall.

Endwall film cooling is difficult because of the strong mainstream impingement and complex vortex structures. Though the research works about film cooling have a long history and related literature are abundant, the endwall film cooling design is still not clear and random to some extent. For some works (Knost and Thole, 2003; Knost, 2003), the main design principles for the endwall film cooling depends on pressure distributions (PD). Liu *et al*. (2020) investigated the full-scale endwall film cooling of a turbine vane with the different design principles. The arrangement ideas of film cooling holes are, respectively, pressure distributions (PD), streamline distributions (SD) and heat transfer coefficient distributions (HTCD). They found the designs based on SD and HTCD have larger coolant coverage and the design based on heat transfer coefficient can effectively reduce the high temperature region.

Constructal structures has been used in the design of cooling structures related to many applications to improve heat transfer and cooling efficiency. Cafiero *et al*. (2016), Cafiero *et al*., 2017) applied a grid geometry, similar to constructal structures, to improve the heat transfer effects of impinging jets. The grid geometry can produce turbulence at multiple scales and can control turbulence level by geometric parameters. This kind of arrangement has extreme benefits to improve the heat transfer purpose.

In the present work, constructal structures are introduced to the design of film cooling holes and four-holes pattern is proposed. The arrangement of film cooling holes is combining constructal structures and distribution principles aiming at improving the overall cooling efficiency and coolant coverage at the tough region, i.e. vane- PS junction region. The distribution principles include pressure coefficient, limiting streamline and heat transfer coefficient distributions proposed in our previous work (Liu *et al*., 2020) and this work is the extension to furtherly improve the overall coolant coverage.

2. Computational domain

The computational domain of the endwall between two vanes is displayed in Figure 1 and related parameters are show in Table 1. The domain is built according to the endwall flow passage with extended channels to develop the flows. The vane file is
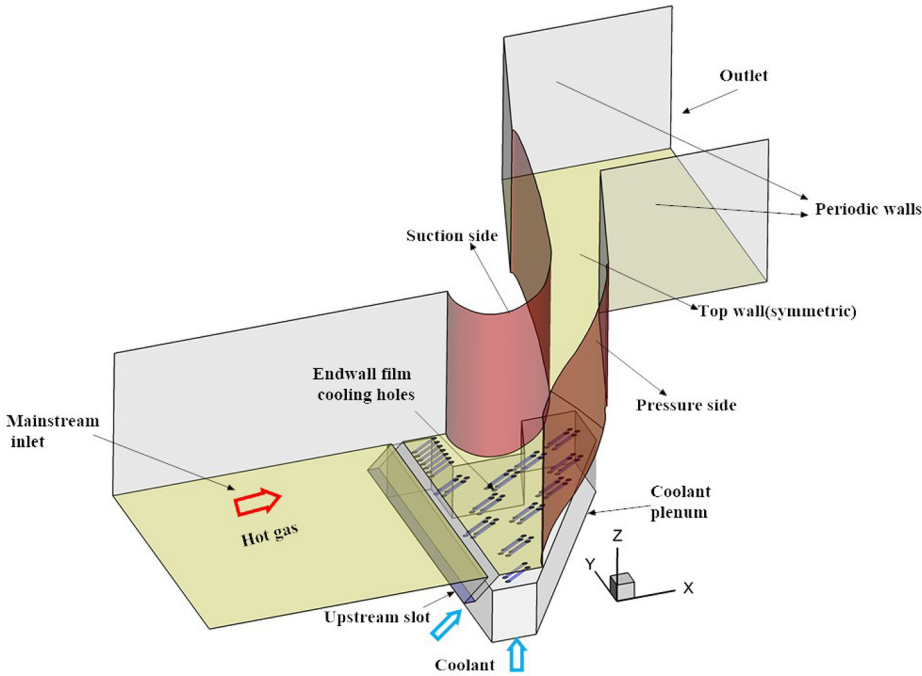
Geometric parameters		Flow conditions	
Scale	9	Inlet Reynolds number	2.2×10^5
Span of the vane	S = 552.42 mm	Inlet mainstream velocity	6.3 m/s
Chord of the vane	C = 594 mm	S	0.5%–1.25%
Pitch between adjacent vanes	P = 457.38 mm	F	0.5%–1.25%
Coolant injection angle	$\alpha = 30°$	Inlet mainstream turbulence intensity	8%

taken from the thesis written by Knost (2003). The vane file is scaled up 9 times in the
real size. The geometry and flow parameters are shown in Table 1. The mainstream
velocity is 6.3 m/s and the Re is about 220,000, the same with the experiments in Knost
(2003). The reference length of the Reynolds number is the length of the vane chord.
Film cooling holes inject at an angle of 30° to supply the coolant flow on the endwall.
The coolant flow is supplied by a plenum to ensure relatively uniform initial flow field.
A rectangular slot, injecting at an angle of 45°, is placed upstream of the endwall to
provide additional protection for the endwall. A similar slot can also be found in Shiau
et al. (2016), Shiau et al. (2019). The distance between the slot and stagnation point is
0.31 C. S and F mean the ratio of coolant mass flow rate from the slot (M_S) and cooling
holes (M_C) to the mainstream mass flow rate, respectively.

$$S = \frac{M_{\mathrm{S}}}{M_{\mathrm{mainstream}}} \tag{1}$$

$$F = \frac{M_{\mathrm{C}}}{M_{\mathrm{mainstream}}} \tag{2}$$

In this work, S and F are ranging from 0.5%–1.25% and effect of S and F are considered, respectively.

Because the cooling flow is still a small portion of the mainstream flow, the design of the cooling holes on the endwall is based on original related fields without the considerations of film cooling effects. Three kinds of distributions are adopted, respectively, pressure, streamline and heat transfer coefficient distributions. Design A and Design B are based on pressure distribution contours in Figure 2. The design baseline for Design A and Design B is also displayed. For Design A, the cooling holes are arranged along the pressure iso-lines with a pitch ratio (*Pc/D*) of 3. Film cooling holes are arranged based on PD have been considered by some previous works (Granser and Schulenberg, 1990; Knost and Thole, 2004). Design B is also based on the PD while the local cooling hole clusters are designed as four-holes type. The design of the four-holes type is based on constructal structures with four cooling holes evenly distributed. The distance between two opposite cooling holes is 4*D*. The introduction of the constructal structures in the arrangement of the film cooling holes aims to control the cooling flows and increase the local coolant coverage. For Design B, the total film cooling holes are 40 and contains 10 film cooling clusters. All the film cooling holes are normal cylindrical holes with an inclination ejecting angle of 30°. The pitch ratio (P_c/D) is 3 and the length ratio (l/D) is 10 for all the designs.

The designs based on the SD and HTCD are displayed in Figure 3, respectively, Design C and Design D. The design baselines of the cooling holes are marked in the figure according to the distributions. The idea of Design D comes from considering coolant overage associated with the corresponding temperature distribution for the arrangement of cooling holes. The film cooling holes for each design based on the constructal structures contain 10 clusters and the total number is 40.
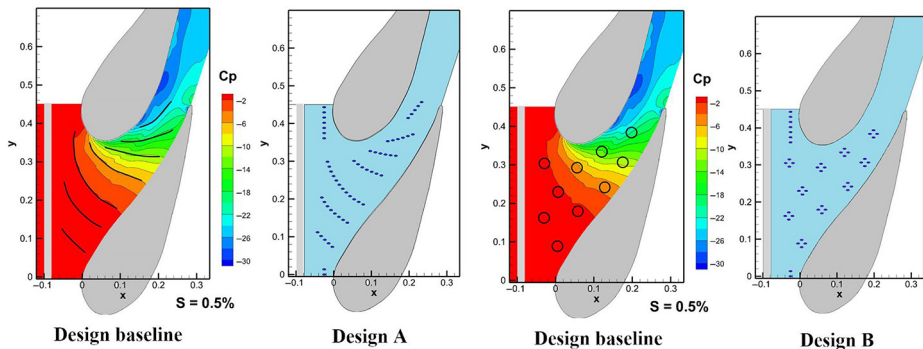
Figure 2.
Endwall film cooling design based on pressure coefficients distribution

Notes: Design A: normal cylindrical holes arranged with pressure iso-lines; Design B: film cooling holes arranged with pressure distribution and fractal theory

3. Computational method

3.1 Turbulence model

Turbulence model selection is very important in dealing with the turbulent flow with complex flow conditions. The k-ω SST model is selected with the advantages of the k-ε and k-ω models and has better performance in dealing with boundary layers. The k-ω SST model has wide applications in simulations related to turbomachinery. Turbulence model validation is provided in Section 3.4.

3.2 Boundary conditions and solver

The mainstream flow condition settings are according to the previous experimental studies (Knost, 2003), which provide conveniences for the turbulence model validations.

The temperature difference of the mainstream hot gas and the coolant is 20 K and the properties of air are assumed to be constant. Therefore, the effect of physical properties related to the temperature difference of the hot and cold gas is not considered in this paper. Based on the previous experiments (Knost, 2003), the mainstream is specified by a velocity of 6.3 m/s and corresponding Reynolds number 2.2×10^5. The inlet is built as an extended channel to develop the inlet flow as a fully-developed flow regime. An outflow is chosen to set the outlet boundary conditions. The height of the computational domain is just half of the vane height. The period side walls are split at the edge of the suction side and the PS to provide an entire flow passage between two vanes. The sidewalls are chosen as periodic walls and the top wall is set symmetric.

Mass flow inlet is set for the upstream slot and the flow rate ratio S ranging from 0.5%–1.25%. The coolant air is supplied from the inlet plenum with flow rate ratios (F) ranging from 0.5%–1.25%. The temperature of the coolant air is 300 K (T_c) with a turbulence intensity of 5%. A little different from the experiment, the mainstream turbulence intensity is set as 8% in the calculations which is based on the engine-representative conditions. The turbulence intensity is set based on the hydraulic diameter. In the turbulence model validation part, the turbulence intensity is set as 1.3%, the same as in the reference (Knost, 2003) for comparisons.

SIMPLEC method is adopted for coupling of pressure and velocity fields. For the spatial discretization, the least squares cell based is chosen for the gradient. The second-order upwind scheme is chosen for the discretization of pressure, momentum, turbulent kinetic energy, specific dissipation rate and energy equations of the k-ω SST model. Residuals and averaged temperature are chosen to determine the calculation convergence. The absolute criteria are set as 10^{-6} for the continuity, x-velocity, y-velocity, z-velocity, k and ω items and an absolute criterion of 10^{-8} is chosen for the energy equation. Besides the residuals, the
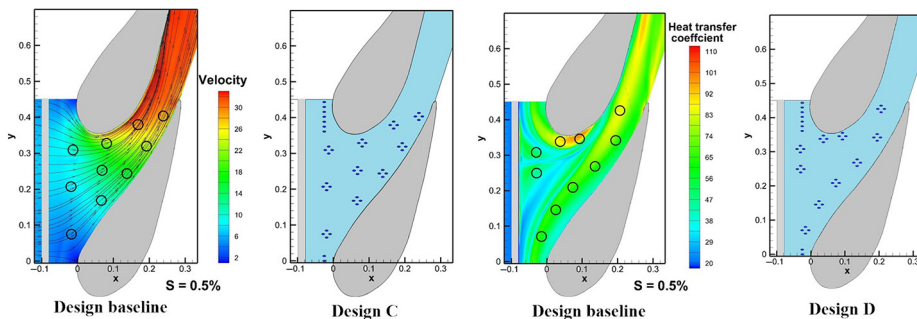
Figure 3.
Endwall film cooling designs based on streamline distribution with fractal theory (Design C) and heat transfer coefficients distribution with fractal theory (Design D)

average temperature on the endwall is also chosen to judge the convergence of the calculations. The average temperature difference of the two judgement is less than 10^{-8}.

3.3 Mesh details

The meshes used in this work are discretized by ANSYS ICEM 19.1. The structured mesh is adopted to ensure computational efficiency and accuracy. The local mesh details are presented in Figure 4. The meshes are dense with a wall distance $y+$ less than 1 in the near-wall region. The boundary layers of the endwall, PS, as well as suction side are well treated because they have a great influence on passage flow development and vortex generation. For the mesh generation, O shape-block, Y shape-block and the discrete block strategy are adopted to improve the quality. For the contacting region, the meshes are denser to ensure that the data transportation is smooth and efficient.

Mesh impendence study is performed based on Design D at $M_C = 0.5\%$ and slot mass flow rate ratio = 0.5%. The results predicted by four mesh systems are provided in Table 2, respectively, having 5.3 million, 7.6 million, 10.2 million and 13.6 million cells. The scale factors of the mesh nodes variations are, respectively, 0.8, 0.9, 1.0 and 1.1. The averaged η of
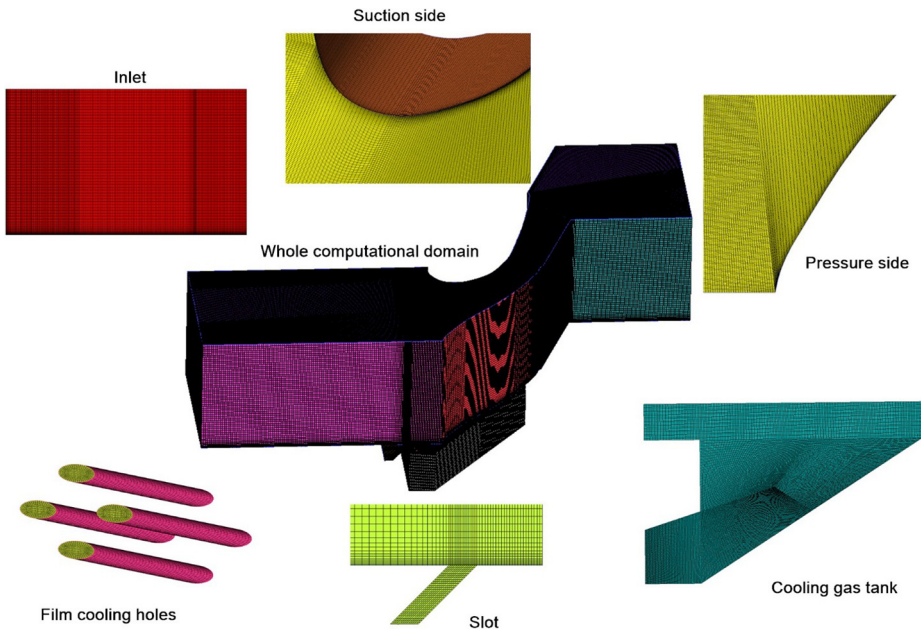

Figure 4.
Structured meshes generated at typical regions of the computational domain

Table 2.
Comparisons of averaged pressure drop and cooling effectiveness

	Scale factor	Total meshes	ΔP(Pa)	η_{avg}
Mesh 1	0.8	5,368,717	396.574	0.214
Mesh 2	0.9	7,631,748	398.132	0.216
Mesh 3	1.0	10,290,464	397.561	0.215
Mesh 4	1.1	13,696,982	399.458	0.219

the endwall and inlet-outlet pressure drop predicted by different mesh systems are both compared. The η is defined as:

$$\eta = \frac{T_w - T_g}{T_c - T_g} \tag{3}$$

From the table, the pressure drop and averaged η predicted by four mesh systems are much close. In addition, the local η contours for Design A calculated by four mesh systems are shown in Figure 5. For the figure, the distribution of contours by different mesh systems are much close to each other. The small difference can be found in the junction regions of the vane and the endwall. According the results in Table 2 and Figure 5, Mesh 3 (about 10.3 million) is used for lateral calculations in the paper.

3.4 Turbulence model validation

The comparison of film cooling contours, the pressure coefficient and endwall heat transfer are also validated in our previous work (Liu et al., 2020). The experimental results is got from Kang et al. (1999).

Figures 6 and 7 provides comparisons of the predicted endwall η contours with the experimental data at S = 0.5% and F = 0.5%–0.75%. The experimental results are from the film cooling arrangement of Ref. (Knost, 2003). The film cooling contours on the endwall
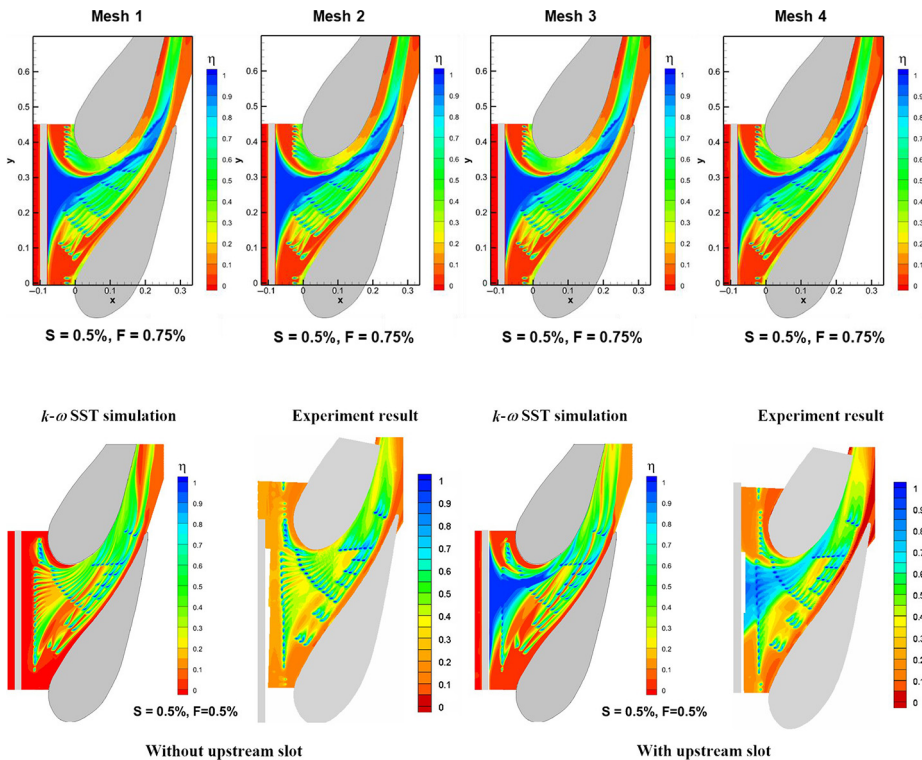

Figure 5.
Mesh independence
study (endwall film
cooling effectiveness
contours for
Design A)

Figure 6.
Turbulence model
validations of
endwall film cooling
effectiveness
comparisons at S =
0.5% and F = 0.5%

with or without the upstream slot are both compared. Overall, the predicted contours of η have good agreements with the experimental results for all cases. Together with the coolant flows from the upstream slot, coolant flows are drawn from the PS to the SS. The junction region of the PS and the endwall has a poor coolant coverage. By the comparison of Figure 5 with Figure 6, it is found that at smaller cooling hole mass flow ratio, i.e. $F = 0.5\%$, the coolant flow on the endwall upstream the LE of the vane has difficulties to be ejected out due to the high pressure in the LE region. Based on the detailed distribution characteristics, the calculations can effectively capture the coolant coverage distribution details on the endwall. Therefore, the k-ω SST model prove to the accuracy in predicting the film cooling flow structures on the endwall. The coolant flow injecting from the upstream slot has benefits in improving the coolant coverage from film cooling holes.

Figure 8 compares lateral η distributions at $S = 0.5\%$ and $F = 0.75\%$ for turbulence model validation. Each data in the figure is obtained by averaging a group of data in the spanwise direction. From the figure, the calculation results predicted by k-ω SST model have good agreements with experiment results, especially in the region of $x/C > 0$. Some deviations can be found in the region with $x/C < 0$. The differences may be caused by the

Figure 7.
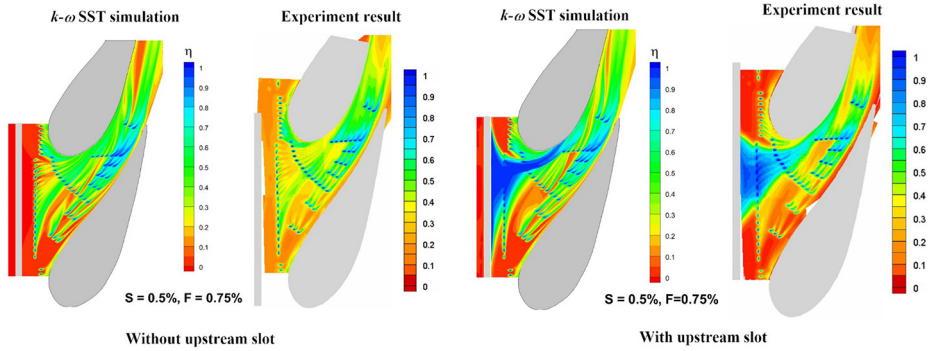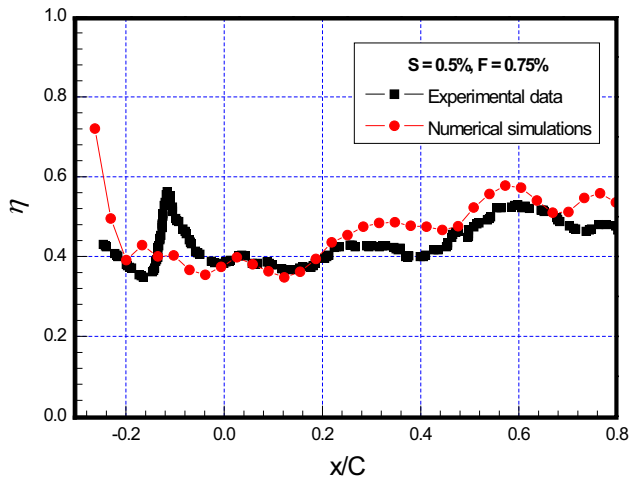Turbulence model validations of endwall film cooling effectiveness comparisons at S = 0.5% and F = 0.75%

Figure 8.
Turbulence model validations of lateral averaged film cooling effectiveness comparisons at S = 0.5% and F = 0.75%

different main flow condition in the experiment and numerical calculations. Compared with the experiment data, the magnitude of averaged film cooling effectiveness and distribution trend predicted by k-ω SST model are acceptable. According to the validated result in Figures 6 to 8, k-ω SST model has provided enough accuracy in predicting the endwall film cooling and can be used in the lateral calculations.

4. Results and discussions

Figure 9 presents the η contours of different designs at different mass flow rate ratios. Two mass flow rate ratios of cooling holes are adopted, respectively, 0.5% and 0.75%. From the figure, the arrangements of the film cooling holes have obvious effects on the coolant coverage on the endwall. With the film cooling holes designed as a four-holes constructal pattern, the coolant flows are well converged and are not affected by the mainstream in the cluster. For the traditional design, i.e. Design A, the film cooling holes are scattered separately in different positions on the endwall, the coolant flows are pushed from the PS to the SS by the mainstream. The coolant protection in the junction region of the PS and the endwall is poor for Design A. For Design B, combining the pressure distribution and four-holes constructal pattern, it provides relatively good coolant coverage, especially at the junction region of the PS and the endwall. Design C, combining the streamline distribution and four-holes pattern, the cooling holes are arranged along the flow path and provide benefits of the coolant coverage on the whole endwall. Also, the coolant coverage in the "tough" region is greatly improved compared with the results in Design A. Design D combines the heat transfer distribution (HTD) and four-holes pattern to remove the high temperature regions because of the strong flow impingement and vortex effect. The cooling
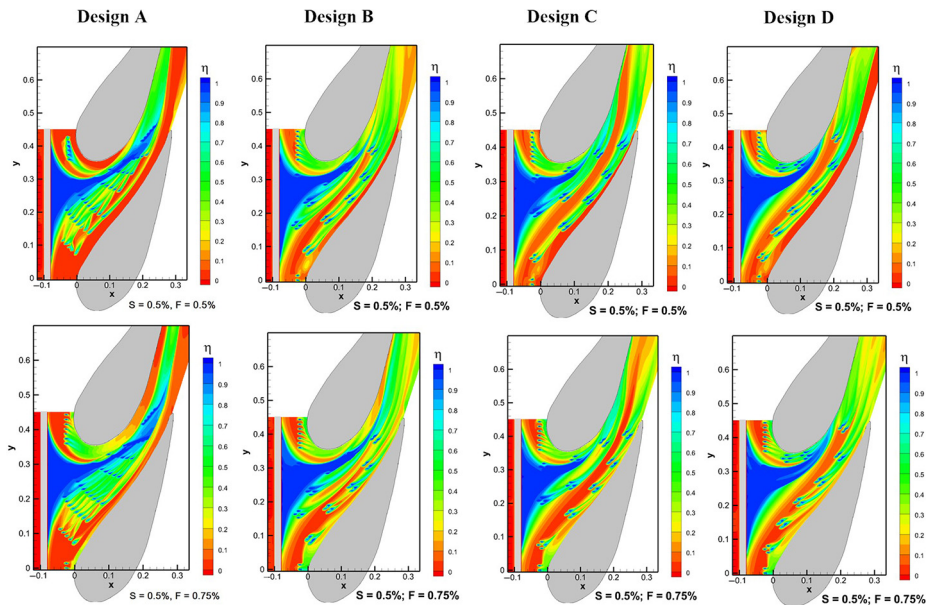
Note: The mass flow rate ratios of cooling holes of 0.5% and 0.75% are provided for comparisons

holes are arranged in the high heat transfer region and provide some convenience for reducing the high temperature region. Also, an improved coolant coverage in Design D is found. Not only the cooling holes arrangement, but also the mass flow rate ratio have great effects on the coolant coverage on the endwall. When the mass flow rate ratio of the film cooling holes (F) is increased from 0.5% to 0.75%, the coolant coverage on the important regions is improved significantly at the LE and PS-endwall junction regions. For Design A, at the smaller mass flow rate ratio, coolant flows upstream of the vane LE have difficulties to be ejected out. However, the LE region can be protected well at a relatively large M_C, i.e. F = 0.75%.

Figure 10 provides the η contours for Design B at different F. The F are ranging from 0.5%–1.25%. From the figure, the mass flow rate ratios have obvious effects on the coolant coverage on the endwall. At the larger mass flow rate ratios, the coolant flows eject from the endwall strongly and impinges on the vane surfaces. The regions, such as the LE endwall and PS-endwall junction regions, are well protected. Therefore, increasing mass flow rate ratio is a good way to enlarge coolant coverage on the endwall. However, when F is too large, more portion of coolant flows directly impinge on the vane surface and coolant coverage of the endwall becomes worse. The selection of F should balance the endwall cooling effect and the junction region of the vane surfaces. Increasing the mass flow rate ratio is a good way to increase the coolant coverage in the tough regions where the coolant flows have difficulties to attach.

Figure 11 displays the η contours for Design B at different mass flow rate ratios of the upstream slot (S). With the larger S, the endwall coolant coverage is effectively enlarged. The coolant flows ejecting from the upstream slot interacts with mainstream flow and is driven from the PS to the SS. Overall, the coolant coverage regions on the junction region of the PS and endwall are almost kept the same with increased mass flow ratios. The increase of the mass flow rate ratio of the upstream slot can increase the coolant coverage on the endwall between two vanes, especially at the downstream region of the slot. Compared with a single cooling hole, a cluster of film cooling holes, i.e. four holes pattern, has benefits to gather the coolant flow and to form effective coolant coverage.

The interaction of coolant flows originating from the slot and the endwall film cooling holes for different designs are shown in Figure 12. The slot mass flow ratio rate (S) and film cooling holes mass flow rate ratio (F) in this figure are, respectively, set as 0.5% and 0.5%. In Design A, the coolant flow has some difficulties to be ejected out from the film cooling holes near the PS. When the film cooling holes is designed as a cluster as shown in Design B, Design C and Design D, the coolant ejection and the coolant coverage are improved. Also,
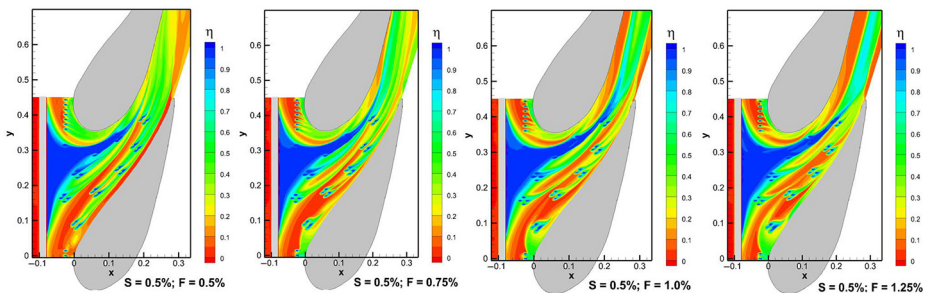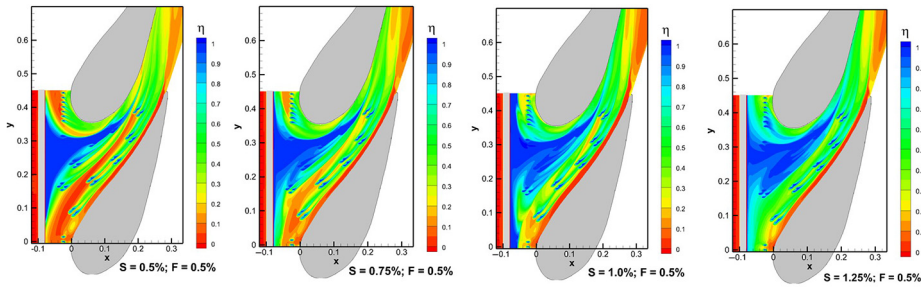

Figure 10.
Film cooling effectiveness contour for the design with pressure distribution and fractal theory (Design B)
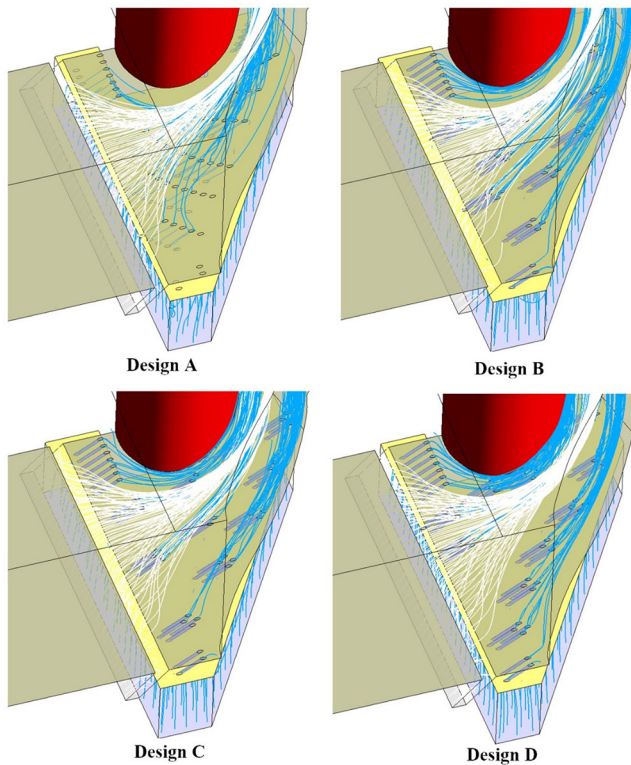
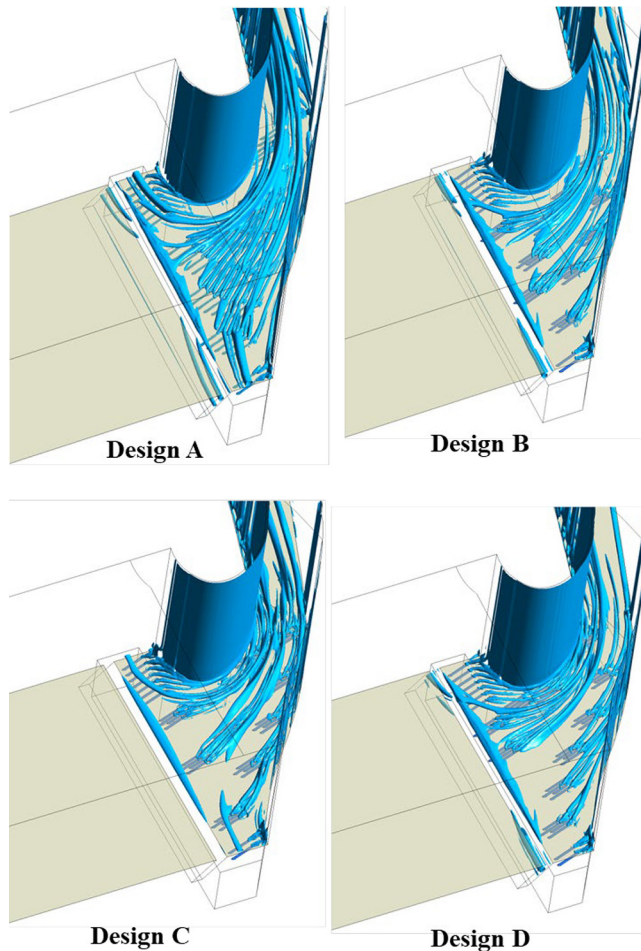**Note:** The film cooling holes mass flow ratio is ranging from 0.5%–1.25%

the coolant ejecting from the cooling holes upstream the LE is improved when cooling holes cluster is used. For Design A, coolant flows have some difficulties to be ejected out from cooling holes on the endwall near the LE region. A larger portion of the coolant flows ejected from the upstream slot gather in the middle region of the flow passage and junction region of the vane-endwall have poor coolant coverage.

Note: The slot mass flow ratio is ranging from 0.5%–1.25%

Design A

Design B

Design C

Design D

Notes: The slot mass flow ratio rate (S) and film cooling holes mass flow rate ratio (F) of the compared cases are respectively set at 0.5% and 0.5%

The vortex structures are in the endwall flow field is displayed in Figure 13. The vortex structures are generated by Q-criterion at S= 0.5% and F = 0.75%. From the figure, the vortices mainly found in the slot coolant injection region, cooling holes injection and wall shear layer. The vortex structures present the secondary flow effects in the flow field and reflect the coolant injection to some extent. Compared with discrete single film cooling hole (Design A), the four-holes patten provides a stronger injection from the film cooling holes near the PS wall where the coolant flow has difficulties to attach because of cross flow effect. The coolant flows impinge on the PS wall and provide coolant coverage on the junction region of PS and endwall. However, the coolant flow ejecting from the discrete cooling hole is easily affected the passage cross flow on the endwall caused by the pressure difference between the PS and the SS.

Note: The vortex structures are displayed by Q-criterion

The velocity distributions on *y-z* sections in the flow passage between two vanes are displayed in Figure 14. Two *y-z* planed are selected, respectively $x = 0$ and $x = 0.5C$. From the figure, it is evident that the mainstream is accelerated by the vane along the flow passage. Near the PS, the velocity is lower than on the SS. Concerning different film cooling holes arrangements, such as Design A and Design B, the mainstream velocity distribution has little difference shown in the figure. The small difference can be found in the vane-endwall junction region. From the PS to the SS, the velocity is gradually increased because of the crossflow effect. Near the endwall or vane surface, the velocity is low due to the strong shear stress. However, the larger flow disturbance and larger shear stress in the regions near the endwall.

Figure 14.
Velocity distributions
on *y-z* sections in the
flow passage between
two vanes
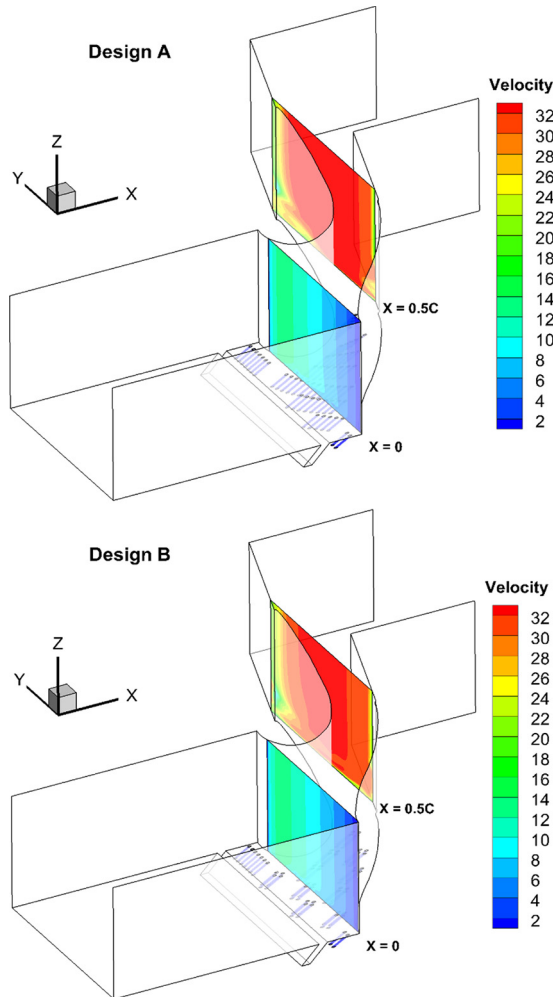
Note: Two y-z sections are selected, respectively
x = 0 and x = 0.5C

Figure 15 displays the laterally averaged η on the endwall at different F. Along the streamwise direction, the averaged η is gradually decreased. When x/C is around 0.5, the averaged η is rapidly decreased. Overall, the film cooling effectiveness is larger at relatively larger film cooling holes mass flow ratio. For Design C, the trend is different and the film cooling effectiveness has no obvious variations with the increased mass flow ratios. Compared with Design A, the film cooling effectiveness of designs based on four holes patterns is greatly improved in the downstream region. Also, the designs based on four holes pattern have relatively high averaged η.

Figure 16 presents the comparisons of laterally averaged η on the endwall for different designs. Every value in x direction is calculated by averaging all the values in y direction. For all the designs, the averaged η has the largest value in the regions close to the stagnation region. The η quickly decreases when x/C is larger than 0.4 where no film cooling holes are placed. From the figure, it is also clear that the F has great effects on the trends of the laterally averaged η. It seems that the designs based four holes constructal pattern are not so affected by the F. However, Design A, based on PD, is much affected by the mass flow ratio and obtains a much larger averaged η at larger mass flow rate ratios.

The laterally averaged η the endwall for different film cooling holes and slot mass flow ratios are compared in Figure 17. The endwall η of Design B is provided in the figure for comparisons. For Design B, the averaged η has no obvious variations affected by F and the distributions are overlapped. However, the mass flow ratios of the slot have obvious effects on the distributions of the averaged η, especially in the regions of $x/C < 0.4$. With the increased
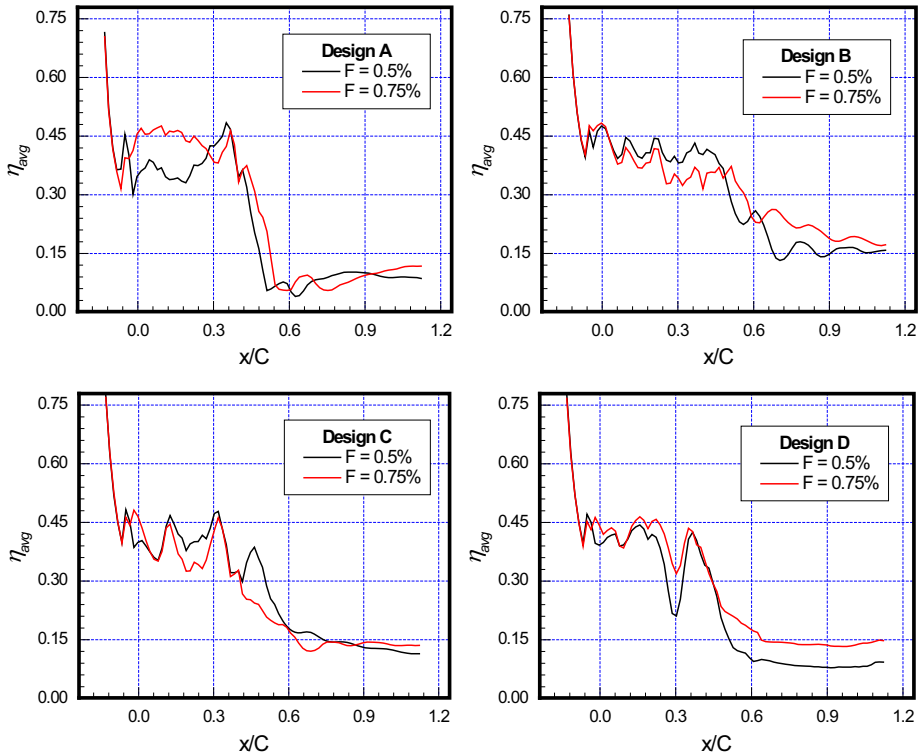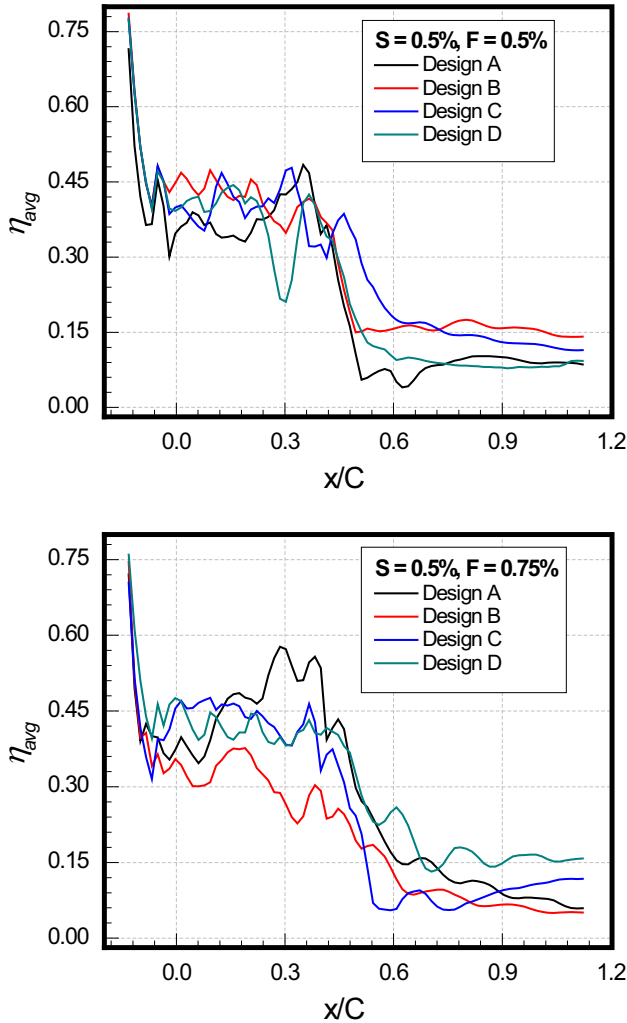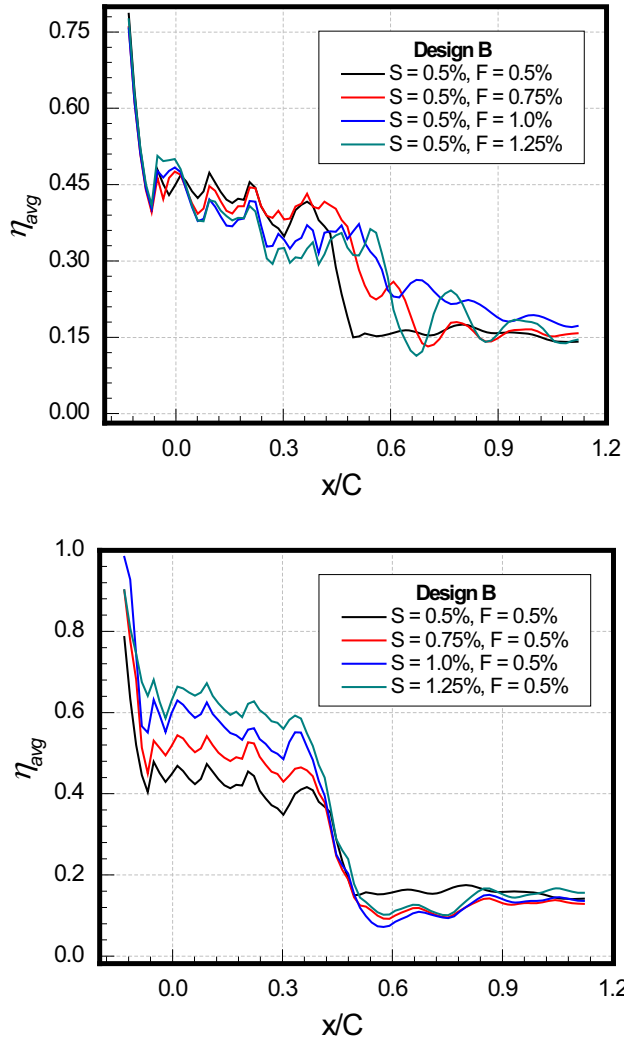

Figure 15.
Lateral averaged film cooling effectiveness on the endwall for different mass flow rate ratios are compared

slot mass flow rate ratios are larger, the averaged η is also increased. However, the coolant flows from the upstream slot mains takes effects in upstream region of the flow passage. In the downstream part of the slot, the effect of mass flow rate ratios of the slot is negligible.

The comparisons of η averaged in different regions are compared in Table 3. The previous Designs I and II and related results are taken from Knost (2003). From this table, it is clear that the designs based on four-holes constructal pattern, i.e. Designs B, C and D, have relatively higher averaged η than the other cases. With the increased F, the averaged η on the PS and SS is also increased. The coolant flows eject from the cooling holes strongly at larger mass flow rate ratios and impinges strongly on the vane surfaces. For the designs based on four-holes constructal pattern, the averaged η on the vane surfaces are also increased quicker than Design A and previous designs. At the small F, the averaged η on

Figure 17.
Lateral averaged film
cooling effectiveness
on the endwall for
different slot mass
flow ratios are
compared

Note: The endwalll film cooling effectiveness of Design B is provided

		Film mass flow rate ratio F = 0.5%			Film mass flow rate ratio F = 0.75%		
		Endwall $\times 10^3$	Pressure side $\times 10^3$	Suction side $\times 10^3$	Endwall $\times 10^3$	Pressure side $\times 10^3$	Suction side $\times 10^3$
	Design A	204.75	0.13	17.27	226.96	23.68	23.11
	Design B	263.39	0.14	26.00	283.96	26.32	35.34
	Design C	260.90	0.69	41.38	245.61	22.89	57.17
Table 3.	Design D	215.29	0.74	40.68	250.89	25.38	59.27
Comparison of film	Previous design I	217.62	0.15	44.46	249.23	24.65	66.27
cooling effectiveness	Previous design II	223.26	13.41	25.49	183.99	42.76	44.76

the vane surfaces is low, especially on the PS. However, the cooling efficiency on the PS is greatly improved at the larger F.

5. Summary and conclusions

This work introduces four-holes constructal pattern into the design of the film cooling holes arrangement on the endwall to improve coolant coverage. Different from traditional design which is based on pressure coefficient distribution, designs based on streamlines and heat transfer distributions are also included. The designs based on four-holes pattern combined with PD, SD and HTCD are, respectively, named Design B, Design C and Design D. Film cooling effectiveness and flow details are analysed and compared. The calculations are performed by k-ω SST model with comprehensive model validations. Some conclusions that emerged from this study are provided below.

For the film cooling cluster with four holes constructal pattern, the ejection of the coolant flow is more strongly and can improve the local coolant coverage. Unlike the traditional Design A, the laterally averaged η of the designs with constructal structures, i.e. Design B, Design C and Design D, are not depending on the mass flow rate ratios of the coolant flows. The designs had advantages in improving the coolant coverage in the "tough" regions, such as the PS and the endwall junction regions.

The design based on streamlines can effectively improve the coolant coverage and the design based on HTD has benefits in reducing the high-temperature regions on the endwall. The four-holes pattern combined with pressure distribution, streamline distribution and HTDs are introduced, and it is found that the overall averaged cooling effectiveness can be further improved. The overall coolant coverage is greatly improved at the larger mass flow rate ratios of the cooling holes. The increase of the slot mass flow rate ratio can improve the coolant coverage at the central region of the flow passage but has no obvious advantages in improving the coolant coverage in the "tough" regions.

References

Cafiero, G., Castrillo, G., Greco, C.S. and Astarita, T. (2017), "Effect of the grid geometry on the convective heat transfer of impinging jets", *International Journal of Heat and Mass Transfer*, Vol. 104, pp. 39-50.

Cafiero, G., Greco, C.S., Astarita, T. and Discetti, S. (2016), "Flow field features of fractal impinging jets at short nozzle to plate distances", *Experimental Thermal and Fluid Science*, Vol. 78, pp. 334-344.

Chen, P., Wang, L., Li, X., Ren, J. and Jiang, H. (2020), "Effect of axial turbine non-axisymmetric endwall contouring on film cooling at different locations", *International Journal of Heat and Mass Transfer*, Vol. 147, p. 118995.

Chen, P., Xue, Q., Li, X., Ren, J. and Jiang, H. (2020), "Full coverage film cooling on a non-axisymmetric contoured endwall and the baseline endwall", *International Journal of Thermal Sciences*, Vol. 158, p. 106562.

Ekkad, S. and Han, J.C. (2013), "A review of hole geometry and coolant density effect on film cooling", *American Society of Mechanical Engineers*, Paper No: HT2013-17250.

Friedrichs, S., Hodson, H. and Dawes, W. (1996), "Distribution of film-cooling effectiveness on a turbine endwall measured using the ammonia and diazo technique", *Journal of Turbomachinery*, Vol. 118 No. 4, pp. 613-621.

Ghosh, K. and Goldstein, R.J. (2011), "Effect of inlet skew on heat/mass transfer from a simulated turbine blade", *American Society of Mechanical Engineers*, pp. 1677-1687.

Granser, D. and Schulenberg, T. (1990), "Prediction and measurement of film cooling effectiveness for a first-stage turbine vane shroud", *American Society of Mechanical Engineers*, Paper No. 90-GT-095.

Han, J.C. and Ekkad, S. (2001), "Recent development in turbine blade film cooling", *International Journal of Rotating Machinery*, Vol. 7 No. 1, pp. 21-40.

Hou, R., Wen, F.B., Cui, T., Tang, X.L. and Wang, S.T. (2019), "Numerical investigation on the improved three-hole cooling unit with the trench", *International Journal of Numerical Methods for Heat and Fluid Flow*, Vol. 29 No. 3, pp. 890-914.

Kang, M.B., Kohli, A. and Thole, K. (1999), "Heat transfer and flow field measurements in the leading edge region of a stator vane endwall", *Journal of Turbomachinery*, Vol. 121 No. 3, pp. 558-568.

Knost, D.G. (2003), "Predictions and measurements of film-cooling on the endwall of a first stage vane", *Virginia Tech*.

Knost, D.G. and Thole, K.A. (2003), "Computational predictions of endwall film-cooling for a first stage vane", *American Society of Mechanical Engineers*, pp. 163-173.

Knost, D. and Thole, K. (2004), "Adiabatic effectiveness measurements of endwall film-cooling for a first stage vane", *American Society of Mechanical Engineers*, pp. 353-362.

Langston, L. (1980), "Crossflows in a turbine cascade passage", *Journal of Engineering for Power*, Vol. 102 No. 4.

Liu, J., Du, W., Hussain, S., Xie, G. and Sundén, B. (2021), "Endwall film cooling holes design upstream of the leading edge of a turbine vane", *Numerical Heat Transfer, Part A: Applications*, Vol. 79 No. 3, pp. 222-245.

Liu, J., Du, W., Zhang, G., Hussain, S., Wang, L., Xie, G. and Sundén, B. (2020), "Design of full-scale endwall film cooling of a turbine vane", *Journal of Heat Transfer*, Vol. 142 No. 2, p. 022201.

Natsui, G., Little, Z., Kapat, J.S. and Dees, J.E. (2017), "Adiabatic film cooling effectiveness measurements throughout multirow film cooling arrays", *Journal of Turbomachinery*, Vol. 139 No. 10, p. 101008.

Nemdili, F., Azzi, A. and Jubran, B.A. (2011), "Numerical investigation of the influence of a hole imperfection on film cooling effectiveness", *International Journal of Numerical Methods for Heat and Fluid Flow*, Vol. 21 No. 1, pp. 46-60.

Oke, R., Simon, T., Shih, T., Zhu, B., Lin, Y.L. and Chyu, M. (2001), "Measurements over a film-cooled, contoured endwall with various coolant injection rates", *American Society of Mechanical Engineers*, Paper No: 2001-GT-0140.

Oke, R.A., Simon, T.W., Burd, S.W. and Vahlberg, R. (2000), "Measurements in a turbine cascade over a contoured endwall: discrete hole injection of bleed flow", *American Society of Mechanical Engineers*, Paper No: 2000-GT-0214.

Shiau, C.C., Chen, A.F., Han, J.C., Azad, S. and Lee, C.P. (2016), "Full-scale turbine vane endwall film-cooling effectiveness distribution using pressure-sensitive paint technique", *Journal of Turbomachinery*, Vol. 138 No. 5, p. 051002.

Shiau, C.C., Sahin, I., Wang, N., Han, J.C., Xu, H. and Fox, M. (2019), "Turbine vane endwall film cooling comparison from five film-hole design patterns and three upstream leakage injection angles", *ASME Journal of Thermal Science and Engineering Applications*, Vol. 13, p. 031012.

Sundaram, N. and Thole, K. (2008), "Bump and trench modifications to film-cooling holes at the vane-endwall junction", *Journal of Turbomachinery*, Vol. 130 No. 4, p. 041013.

Sundaram, N. and Thole, K. (2009), "Film-cooling flow fields with trenched holes on an endwall", *Journal of Turbomachinery*, Vol. 131 No. 4, p. 041007.

Wang, N., Zhang, M., Shiau, C.C. and Han, J.C. (2019), "Film cooling effectiveness from two-row of compound angled cylindrical holes using PSP technique", *Journal of Heat Transfer*, Vol. 141 No. 4, p. 042202.

Yang, X., Liu, Z., Zhao, Q., Liu, Z., Feng, Z., Guo, F., Ding, L. and Simon, T.W. (2019), "Conjugate heat transfer measurements and predictions for the vane endwall of a high-pressure turbine with upstream purge flow", *International Journal of Heat and Mass Transfer*, Vol. 140, pp. 634-647.

Zhang, L.J. and Jaiswal, R.S. (2001), "Turbine nozzle endwall film cooling study using pressure sensitive paint", *Journal of Turbomachinery*, Vol. 123 No. 4, pp. 730-738.

Zhang, G.H., Liu, X.T., Sunden, B.A. and Xie, G.N. (2019), "Computational analysis of span-wise hole locations on fluid flow and film cooling of internal channels with crescent ribs", *International Journal of Numerical Methods for Heat and Fluid Flow*, Vol. 29 No. 8, pp. 2728-2753.

Corresponding authors
Bengt Ake Sunden can be contacted at: bengt.sunden@energy.lth.se and Wenxiong Xi can be contacted at: 13739076081@163.com